Thai Journal of Mathematics
Volume 8 (2010) Number 1 : 197–214
www.math.science.cmu.ac.th/thaijournal
Online ISSN 1686-0209

A Numerical Study of Two Coordinates for Energy Balance Equations by Wave Model

W. Wannawong†, U.W. Humphries, P. Wongwises,
S. Vongvisessomjai and W. Lueangaram

Abstract : For the numerical simulations of the ocean wave model, the coordinates for the operation of wave prediction model need to be studied due to the high resolutions affecting the domain boundaries. In the present study, the two coordinates for the wave energy balance equations required for operation and computation are proposed. The two–dimensional models, the spherical coordinate and Cartesian coordinate propagations with deep and shallow water conditions, are used to test the operation of the wave model from the eye storm generation at the Pacific Ocean entering into the South China Sea (SCS) and the Gulf of Thailand (GoT) respectively. The results suggest that the spherical coordinate propagations with deep water conditions are acceptable with similar values of the observational data.

Keywords : Cartesian coordinate, Energy balance equations, spherical coordinate, Wave model.
2000 Mathematics Subject Classification : 81T80, 91B76, 91B74.

1 Introduction

In the design of computational coordinates to study the storm waves, it is important to compute the regional wave conditions. The ocean waves propagate from the eye storm generation at the Pacific Ocean entering into the South China Sea (SCS) and the Gulf of Thailand (GoT) and change their heights, lengths and directions according to the particular bathymetry and the presence of currents and structures [19]. Shoaling, refraction, diffraction, reflection and wave breaking may

The authors would like to acknowledge the Commission on Higher Education for giving financial support to Mr.Worachat Wannawong under the Strategic Scholarships Fellowships Frontier Research Networks (CHE–PhD–THA–NEU) in 2007.

all occur. Since the ocean waves are random, accurate prediction of their transformation by these combined processes is difficult. Several theories and models have been applied to study the regional waves such as the GoT (Figure 1) and each theory and model has certain advantages and limitations with respect to its applicability.

The purpose of the present work is to study the formulation of the wave energy balance equations and its applications in the two–coordinates. The two–coordinates; the spherical and Cartesian coordinates are applied to study in the GoT in a case study of Typhoon Linda 1997 by the third generation WAve Model Cycle 4 (WAMC4)[14, 5]. The spherical coordinates in the coarse grid domain (CGD) and fine grid domain (FGD) with deep water conditions are adopted from researches of Vongvisessomjai [16, 17] and Meteorological Division, Hydrographic Department, Royal Thai Navy, Sattahip, Chonburi, Thailand. In the present study, the two–coordinates of the WAMC4 model are exhibited the spherical coordinate in the CGD with the Cartesian coordinate in the FGD under the shallow water condition as the first experiment. For the second experiment, the spherical coordinate in the CGD with the spherical coordinate in the FGD are studied under the deep water condition. The CGD covering from $95°E$ to $155°E$ in longitude and from $20°S$ to $40°N$ in latitude and the FGD covering from $99°E$ to $111°E$ in longitude and from $2°N$ to $14°N$ in latitude are applied to both experiments. The both experiments with the nested grid technique are calculated by the WAMC4 model which is shown in Figure 1. The outline of this work is as follows: Section 2 gives a description of the numerical models; Section 3 presents the implementation of the models and experimental designs; Section 4 shows the results of experiments; and Section 5 presents the discussions and conclusion.

2 The Numerical Models

The numerical models used in the present study have been used operationally in this section. The WAve Model Cycle 4 (WAMC4) is now one of the most extensively tested third–generation wave model in the world and its performance on global, regional and coastal scales [12] is well known [14, 5, 3]. In this section, a review of the numerical schemes and their numerical characteristics are described.

2.1 The Wave Model

The WAMC4 model solves the energy balance equation in the regional scale with terms of the discrete energy density[1], $F(\theta, f; \mathbf{x}, t)$, where t represents time, $\mathbf{x}$ represents the geographical space in Cartesian (x, y) or spherical (λ, ϕ) coordinates, and (θ, f) represent the spectral space (direction and frequency, respectively). The wave direction θ represents the wave direction measured clockwise from the true north. Excluding the intrinsic frequency, σ, as a coordinate allows the model to overcome the problem of high frequency waves propagating on strong opposite currents (e.g. the absence of diffraction and currents for the coastal scale).

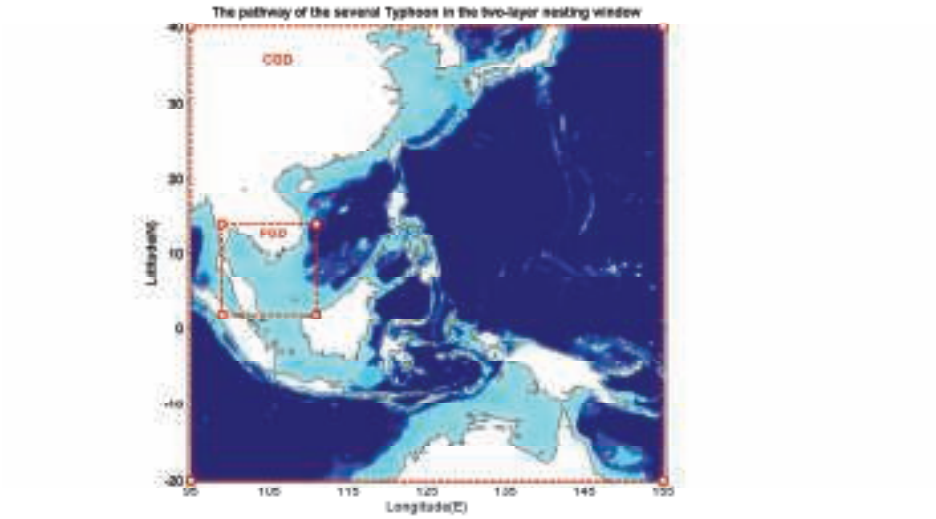

Figure 1: Two experiments of the two coordinates calculated by the nested grid technique of the WAMC4 model.

The WAMC4 model is initially developed to forecast wave conditions on global or regional scales, so it allows the use of spherical or Cartesian coordinates. The governing equation in Cartesian coordinates (x, y) reads,

$$\frac{\partial F}{\partial t} + \frac{\partial c_{g,x} F}{\partial x} + \frac{\partial c_{g,y} F}{\partial y} + \frac{\partial c_\theta F}{\partial \theta} = S_{tot} \tag{2.1}$$

where the propagation speed in the different spaces; $c_{g,x}, c_{g,y}$, and c_θ are given by [13, 6],

$$c_{g,x} = \dot{x} = \frac{dx}{dt} = \sqrt{gd}, \tag{2.2}$$

$$c_{g,y} = \dot{y} = \frac{dy}{dt} = \sqrt{gd}, \tag{2.3}$$

$$c_\theta = \dot{\theta} = \frac{d\theta}{dt} = \frac{1}{k}\Big[\frac{\partial f}{\partial d}\frac{\partial d}{\partial m}\Big]. \tag{2.4}$$

In the equations (2.2), (2.3) and (2.4) for the shallow water condition, g and d represent the gravitational acceleration and the total water depth, k and m

[1] It is worth to remark that the letter F is used to denote the discrete representation of the wave energy density, E.

represent the wave number and the space coordinate in the θ direction, respectively.

The governing equation for the WAMC4 model on the spherical coordinates (λ, ϕ) reads,

$$\frac{\partial F}{\partial t} + \frac{\partial c_{g,\lambda} F}{\partial \lambda} + (\cos\phi)^{-1} \frac{\partial c_{g,\phi}(\cos\phi) F}{\partial \phi} + \frac{\partial c_\theta F}{\partial \theta} = S_{tot} \tag{2.5}$$

where the propagation speed in the different spaces; $c_{g,\lambda}, c_{g,\phi}$, and c_θ are given by,

$$c_{g,\lambda} = \dot{\lambda} = \frac{d\lambda}{dt} = (c_g \sin\theta)(R\cos\phi)^{-1}, \tag{2.6}$$

$$c_{g,\phi} = \dot{\phi} = \frac{d\phi}{dt} = (c_g \cos\theta) R^{-1}, \tag{2.7}$$

$$c_\theta = \dot{\theta} = \frac{d\theta}{dt} = (c_g \sin\theta \tan\phi) R^{-1}. \tag{2.8}$$

Here $c_g = g/2\omega = g/2(2\pi f) = g/4\pi f$ denotes the group velocity of the deep water condition, g represents the gravitational acceleration, ω represents the angular frequency, f represents the frequency, and R represents the radius of the earth, respectively.

At the right hand side of the equations (2.1) and (2.5), S_{tot} is the function representing the source and sink functions, and the conservative non–linear transfer of energy between wave components. For the present applications, the surface wave model included the standard WAMC4 formulations for the S_{tot} terms; wind input S_{in}, non–linear quadruplet wave–wave interactions S_{nl}, whitecapping dissipation S_{ds}, and bottom friction dissipation S_{bf}. For the complete explanation on the physics included in S_{tot}, the reader is referred to Komen et al., [3] and references in there.

The wind input formulation is based on the resonant interaction between the wave induced pressure fluctuations and the waves (Miles' theory). This source of energy is represented as,

$$S_{in} = \gamma F \tag{2.9}$$

where γ is the growth rate of the waves, also called Miles' wave growth mechanism. In WAMC4 model, this term is based on the theory proposed by Janssen [11]. According to Janssen [11], the interphase atmosphere–ocean represents a coupled system where the growth rate of waves depends on the wind, whose profile depends on the sea state. In WAMC4 model, γ is expressed as,

$$\gamma = \max\left[0, (\rho_a/\rho_w)\beta X^2\right] \quad ; \quad X = (u^*/c)\cos\vartheta \tag{2.10}$$

where ρ_a is the density of air, ρ_w is the density of sea water, ϑ is the relative direction between wind and waves, $u^* = \sqrt{\tau/\rho_a}$ is the friction velocity where τ is the wind stress, c is the phase velocity of the waves, and β (the Miles' parameter) is given by,

$$\beta = (1.2/\kappa^2)\nu \ln^4 \nu \quad ; \quad \nu = \frac{g z_e}{(\kappa c_p)^2} \exp(\kappa/X) \tag{2.11}$$

where z_e represents the effective roughness length, c_p is the wave propagation speed and $\kappa = 0.41$ is the von Kármán constant. The nonlinear resonant interaction between the quadruplet of wave components is included in the WAM through an approximation to the exact expression,

$$S_{in}^{exact}(\mathbf{k_4}) = \int \omega_4 \varsigma \delta(\mathbf{k}_1 + \mathbf{k}_2 - \mathbf{k}_3 - \mathbf{k}_4)\delta(\omega_1 + \omega_2 - \omega_3 - \omega_4) \times [n_1 n_2 (n_3 + n_4) - n_3 n_4 (n_1 + n_2)] d\mathbf{k}_1 d\mathbf{k}_2 d\mathbf{k}_3 d\mathbf{k}_4, \quad (2.12)$$

where $n_j = F(k_j)/\omega_j$ is the action density and the coefficient ς is the coupling coefficient. The approximation included in the WAM (DIA method, Hasselmann et al., [15]) reduces the space of resonant quadruplets to a two–dimensional plane where the discrete interaction of a symmetric pair of configurations is only used (see Figures 3.1 and 3.2 in van Vledder [4]).

On finite–depth waters, the computation of S_{nl} is carried out in similar way as on the deep waters, but including a scaling factor:

$$S_{nl} = \Upsilon(\bar{k}H) S_{nl}. \quad (2.13)$$

In equation (2.13), $\bar{k} = [E_{tot}^{-1} \int F(f,\theta) k^{-1/2} df d\theta]^{-2}$ is the mean of wave number, E_{tot} is the total of wave energy density and the scaling factor Υ reads,

$$\Upsilon(\chi) = 1 + \frac{5.5}{\chi}\Big(1 - \frac{5\chi}{6}\Big) \exp\Big(-\frac{5\chi}{4}\Big), \quad (2.14)$$

with $\chi = (3/4)\bar{k}H$.

The term representing the energy dissipation by wave breaking on the deep waters (also called the whitecapping) is based on a extension of the formulation proposed by Komen et al., [2]. In Komen's formulation, the existence of an equilibrium solution of the energy balance equation during fully developed sea condition is assumed. Once the Janssen's theory for the wave growth by sea–atmosphere coupling was implemented, the Komen's formulation had to be extended in order to obtain the proper balance during fully developed sea conditions. In WAMC4 model, the term S_{ds} is evaluated as,

$$S_{ds} = -C_{d1} \bar{\omega} \bar{k}^4 E_{tot}^2 \Big[(1 - C_{d2})(k/\bar{k}) + C_{d2}(k/\bar{k})^2\Big] F, \quad (2.15)$$

where E_{tot} is the total energy, $C_{d1} = 4.5$, and $C_{d2} = 0.5$.

In shallow the water, the both equations need to be extended to include the additional source function S_{bf} representing the energy loss due to bottom friction and percolation. The bottom friction dissipation term, S_{bf} , is represented according to the formulation proposed during JONSWAP (Hasselmann et al., [8]),

$$S_{bf} = -\frac{\Gamma}{g^2} \frac{\omega^2}{\sinh^2 kD} F. \quad (2.16)$$

with $\Gamma = 0.038$, ω is the angular frequency ($\omega^2 = gk \tanh kD$), g is the gravitational acceleration, k is the wave number and D is the finite depth dispersion relation.

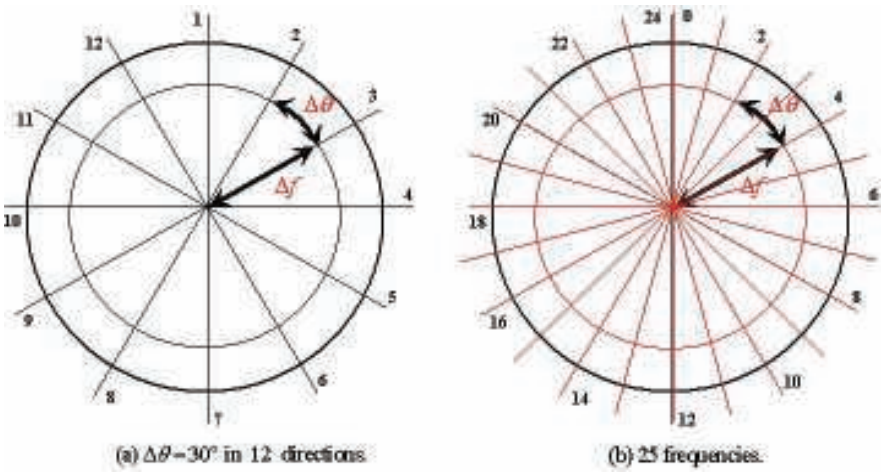

Figure 2: Discrete (a) spectral space possesses 25 frequencies with (b) standard directional resolution 30 degrees in 12 directions.

2.2 Numerical scheme

In WAMC4 model, the spectrum F is represented by a discrete number of frequency bins, $\omega = 2\pi f$, traveling in a discrete number of directions, θ. The standard directional resolution is 30 degrees in 12 directions ($\Delta\theta = 30$), with an azimuthal distribution, whereas the discrete spectral space possesses 25 frequencies, ranging from 0.041Hz to 0.41Hz. The directional components are defined at the directional fragments (staggered points) as shown in Figure 2. The reason of this definition is connected with the advection term. The frequency distribution is logarithmic,

$$f_{n+1} = 1.1 f_n \ , \ n = 0, 1, 2, 3, \ldots 24. \tag{2.17}$$

so that,

$$\Delta f / f = 0.1. \tag{2.18}$$

In the frequency space, the energy distribution is computed according to the physics included in the equations (2.1) and (2.5). Beyond the prognostic region, a diagnostic part is added to the spectrum. The energy distribution in the diagnostic region is given by,

$$F(f > f_{hf}, \theta) = F(f_{hf}, \theta)\Big(\frac{f}{f_{hf}}\Big)^{-5}. \tag{2.19}$$

The dynamic limit for the prognostic region is computed by,

$$f_{hf} = \min\{f_{\max}, \max(2.5\bar{f}, 4 f_{PM})\}, \tag{2.20}$$

where $f_{\max} = (1.1)^{24} f_{\min}$, $\bar{f}$ is the mean frequency, and $f_{PM}$is the peak frequency of the corresponding Pierson–Moskowitz spectrum. The model uses two time steps; one of them is computed according to the Courant–Friedrichs–Lewy (CFL) stability condition, typically assumed as a time step for the propagation, $\Delta t_p \leq (\sqrt{\Delta x + \Delta y})/c_{g(max)}$, and a time step for the source term, Δt_s, which is restricted to be shorter than or equal to the propagation time step. A zero energy flux condition is imposed at coastlines and the possibility of imposing a time dependent condition at open boundaries is also included.

2.3 Wave Propagation

The advection of wave energy is computed by using a forward in time, a first–order upwind differences (explicit) scheme in control volume form. At this stage, the equation (2.1) is solved as an action conservation equation (as mentioned above, S_{tot} is evaluated in the different step). The differences scheme is expressed as,

$$\begin{aligned}\Big[\frac{F^{n+1}-F^n}{\Delta t_p}\Big]_{i,j,k} &= -\Big[\frac{(c_{g,x}F)_{i+1/2}-(c_{g,x}F)_{i-1/2}}{\Delta x}\Big]^n_{j,k} \\ &\quad -\Big[\frac{(c_{g,y}F)_{j+1/2}-(c_{g,y}F)_{j-1/2}}{\Delta y}\Big]^n_{i,k} \\ &\quad -\Big[\frac{(c_\theta F)_{k+1/2}-(c_\theta F)_{k-1/2}}{\Delta \theta}\Big]^n_{i,j}, \end{aligned} \tag{2.21}$$

where (i, j) denote the position in longitudinal and latitudinal directions, respectively, and (k) denotes the spectral–space position (direction). The resolution of the discrete representation of F is given by $\Delta(x, y, \theta)$.

The fluxes on the control volume faces are given by,

$$\begin{aligned}\Big[(c_\zeta F)\Big]^n_{r+1/2} &= 0.5\Big\{\Big[(c_\zeta)_{r+1/2}-|(c_\zeta)_{r+1/2}|\Big]F^n_{r+1} \\ &\quad +\Big[(c_\zeta)_{r+1/2}+|(c_\zeta)_{r+1/2}|\Big]F^n_r\Big\}, \end{aligned} \tag{2.22}$$

$$\begin{aligned}\Big[(c_\zeta F)\Big]^n_{r-1/2} &= 0.5\Big\{\Big[(c_\zeta)_{r-1/2}-|(c_\zeta)_{r-1/2}|\Big]F^n_r \\ &\quad +\Big[(c_\zeta)_{r-1/2}+|(c_\zeta)_{r-1/2}|\Big]F^n_{r-1}\Big\}, \end{aligned} \tag{2.23}$$

with ζ represents the coordinate (x, y, θ) of wave propagation speeds $(c_{g,x}, c_{g,y}, c_\theta)$ and r its corresponding index (i, j, k). The control volume face velocities, $(c_\zeta)_{r+1/2}$ and $(c_\zeta)_{r-1/2}$, whose expressions are given by the equations (2.2)–(2.4), are computed as

$$(c_\zeta)_{r+1/2} = 0.5\Big[(c_\zeta)_{r+1}+(c_\zeta)_r\Big], \tag{2.24}$$

$$(c_\zeta)_{r-1/2} = 0.5\Big[(c_\zeta)_r+(c_\zeta)_{r-1}\Big]. \tag{2.25}$$

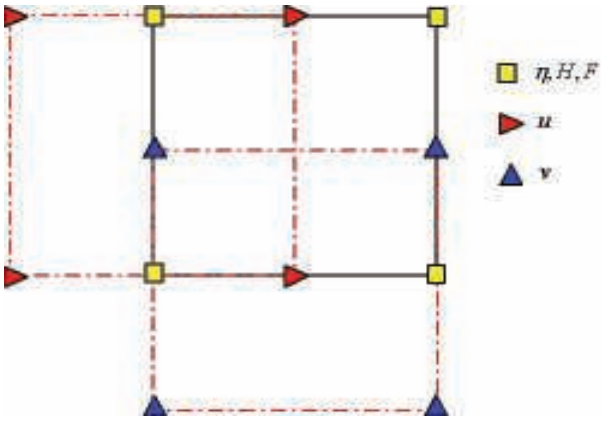

Figure 3: Staggered C–type grid used by the hydrodynamic model [19]. The WAMC4 model uses an A–type grid, in such a way that the governing equation for the wave evolution is computed at points corresponding to elevation values in the hydrodynamic model.

Central differences are used to solve the spatial derivatives of u, v, and d in the equations (2.2)–(2.4) which is neglected the effect of current (u, v) on a staggered C–grid (see Figure 3), and these terms are not computed at points beside the coast. It is worth noticing, u is the velocity in x–longitude direction, v is the velocity in y–latitude direction, and d is the total water depth ($d = \eta + H$) where η is the sea surface elevation and H is the local depth at the mean sea level (MSL).

2.4 Source term integration

The evolution of the source term is computed by a semi–implicit second order method (Leapfrog scheme). After the solution of the equation (2.21), the new spectrum at the points (i, j, k) is modified by the source terms according to,

$$F^{n+1}_{i,j,k} = F^{n}_{i,j,k} + \Delta t_s[(1-\alpha)S^{n}_{i,j,k} + \alpha S^{n+1}_{i,j,k}], \tag{2.26}$$

where i and j denote the position in geographical space, k represents the position in the wave direction space and α is in the range of 0 to 1. None of the source terms $S^{n+1}_{i,j,k}$ depend linearly on $F^{n+1}_{i,j,k}$. Therefore, the Taylor's series expansion is introduced,

$$S^{n+1}_{i,j,k} = S^{n}_{i,j,k} + \frac{\partial S^{n}_{i,j,k}}{\partial F_{i,j,k}} \Delta F_{i,j,k} + ..., \tag{2.27}$$

where the functional derivative in the equation (2.27) can be expressed as a matrix with a diagonal part, $\Lambda^{n}_{i,j,k}$, and a non–diagonal residual. By considering only the

diagonal matrix $\Lambda^n_{i,j,k}$, the equation (2.26) can be expressed as,

$$F^{n+1}_{i,j,k} = F^n_{i,j,k} + \Delta t_s S^n_{i,j,k}[1 - \alpha \Delta t_s \Lambda^n_{i,j,k}]^{-1}. \quad (2.28)$$

In the standard WAMC4 formulation, α is set as 0.5. A limiter on the increments in wave energy is imposed (see discussion in Monbaliu et al., [7]). The limiter is introduced that

$$(\Delta_s F)^n_{max} = 3 \times 10^{-7} g \tilde{u}^*_a f_c f^{-4} \Delta t_s, \quad (2.29)$$

where g is the gravity acceleration, $f_c = f_{max}$ is the cut–off frequency, and

$$\tilde{u}^*_a = \max(u^*_a, g f^*_{PM}/f). \quad (2.30)$$

with u^*_a the air friction velocity and $f^*_{PM} = 5.6 \times 10^{-3} s^{-1}$ the dimensionless Pierson–Moskowitz peak frequency.

As mentioned above, the numerical scheme implemented in the original WAMC4 code is an explicit one, in such a way that the stability of the numerical scheme is determined by the Courant–Friedrichs–Lewy (CFL) condition. More details of the information about the theory and the formulation of spherical coordinates of the WAM model can be found in the WAMDI Group [14].

3 Model Settings and Experimental Designs

3.1 Model Settings

The computational storm waves of from the eye storm generation at the Pacific Ocean entering into the SCS and the GoT were configured with high resolutions. In order to resolve the regional sea waves in the GoT and its surrounding water, two nested domains (Figure 1) with the inside domain (FGD) imbedded into the outside domain (CGD) by one way nested grid were employed for this study. The CGD was set up to cover the storm generations from $95°E$ to $155°E$ in longitude and from $20°S$ to $40°N$ in latitude ($0.5° \times 0.5°$ spatial grid size), which gave 121×121 points for both latitude and longitude. The FGD was covered from $99°E$ to $111°E$ in longitude and from $2°N$ to $14°N$ in latitude ($0.25° \times 0.25°$ spatial grid size), which gave 49×49 points for both latitude and longitude. The propagation and source time step of the CGD were 1800 s and 1800 s respectively while those of the FGD were 600 s and 600 s respectively.

The bottom topography was obtained from GEODAS (available online from http://www.ngdc.noaa.gov/mgg/gdas). The original version (1993), ETOPO5 [9], on a 5–minute latitude/longitude grid (1 minute of latitude = 1 nautical mile, or 1.853 km) was updated in June 2005 for the acceptably deep water. It has been applied in the CGD. The latest version (on July 28, 2008), ETOPO1 [1], on a 1–minute latitude/longitude grid for the high resolution was available in Ice Surface (top of Antarctic and Greenland ice sheets) and Bedrock (base of the ice sheets) versions. The ETOPO1 (Bedrock version) was chosen to apply in the FGD. The

details of the coupled topographies and nested grid domains were described by Xia et al., [10].

The WAMC4 model required the input wind fields and bathymetry data for each nested grid. The wind fields at a height of 10 m were obtained from the U.S. Navy Global Atmospheric Prediction System (NOGAPS) which is a global atmospheric forecast model [18] with $1^\circ \times 1^\circ$ data resolution and the linear interpolation was used to generate the wind data to the grid points. The bathymetry data was extracted from ETOPO5 in the updated version and ETOPO1 [1].

The results of WAMC4 model were exposed in every hour of Typhoon Linda passing through the GoT. The stability of model was computed according to the CFL stability condition.

3.2 Experimental Designs

In order to compute the storm wave on the surface wave layer, two experiments were conducted in this study (Table 1). The WAMC4 model run by the nested grid which modified the spherical coordinate propagation with deep water (shallow water flag condition) in the CGD and Cartesian coordinate propagation with shallow water (shallow water flag condition) in the FGD was referred to as Exp.I. In Exp.II, the WAMC4 model run with deep water condition in the spherical coordinate propagation was provided to the FGD and the same condition with Exp.I was used for the CGD.

Table 1: Details and reference codes of the numerical experiments

Experimental code	Numerical experiments with water flag conditions	
	Coarse Grid Domain (CGD)	Fine Grid Domain (FGD)
Exp.I	Spherical coordinates in Deep water	Cartesian coordinates in Shallow water
Exp.II	Spherical coordinates in Deep water	Spherical coordinates in Deep water

4 Results of Experiments

The simulations of storm wave and propagation were analyzed from a set of model experiments: Exp.I and Exp.II as described in Table 1.

The computation of wave height generated by Typhoon Linda using the WAMC4 model (Exp.I) was firstly considered. The maximum significant wave heights related with the maximum wind fields in the CGD and FGD during the passage of Typhoon Linda are shown in Figures 4–6. The WAMC4 model of both experiments was run with the same wind field (wind speed), domain (wind fetch) and the same time (duration) but different coordinate propagation and flag conditions. Figures 5(a) and (b) showed the wave height at the same location with different coordinate propagations and flag conditions in Exp.II. The effect of coordinate

propagation and flag condition (deep water) on wave height can be easily considered from Figures 5(b) and 6(b), which showed the wave height increased with increasing water depth. In addition, Super Typhoon Keith 1997 was found in the CGD used in this study.

To quantify the effects of extreme of wave height and the difference between the maximum wave heights computed by the WAMC4 model at four locations of buoy in the GoT region (Figure 7 and Table 2) were calculated. The differences of wave heights at each station were presented in Table 3. The results showed that the wave heights at stations I, II and III were similarly different while station IV showed a markedly different wave height.

Table 2: Computational and observation points for the WAMC4 model simulations

Station code	Station name	Station point	Computational point
I	Ko Chang	$102.20^\circ E$ $12.00^\circ N$	$102.25^\circ E$ $12.00^\circ N$
II	Rayong	$101.22^\circ E$ $12.44^\circ N$	$101.25^\circ E$ $12.50^\circ N$
III	Huahin	$100.17^\circ E$ $12.44^\circ N$	$100.25^\circ E$ $12.50^\circ N$
IV	Satun based weather	$101.42^\circ E$ $9.28^\circ N$	$101.50^\circ E$ $9.25^\circ N$

Table 3: Comparison of the maximum wave height (m) of the WAMC4 model with the observations

Station code	Station name	Exp.I (m)	Exp.II (m)	Observation (m)
I	Ko Chang	1.67	2.22	2.50
II	Rayong	1.54	2.52	2.97
III	Huahin	1.60	2.67	4.06
IV	Satun based weather	2.30	2.42	12.48

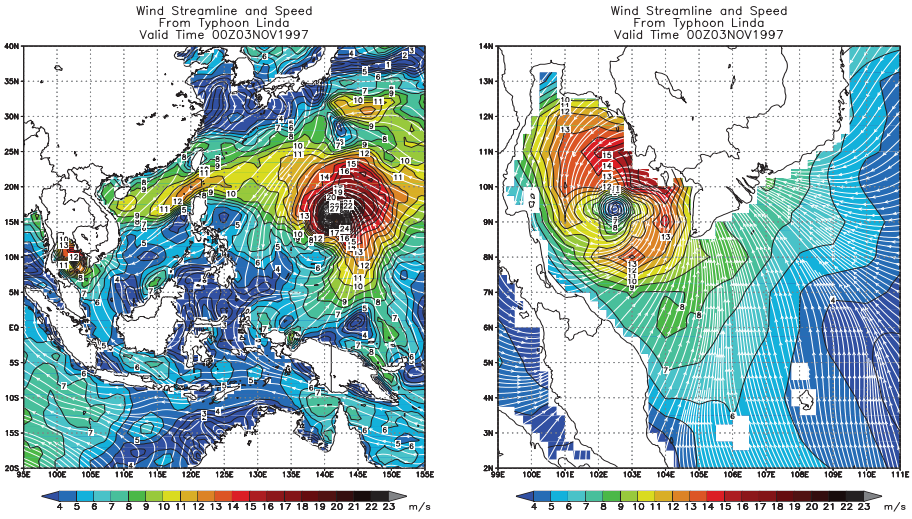

(a) (b)

Figure 4: The maximum wind field in (a) the CGD and (b) the FGD.

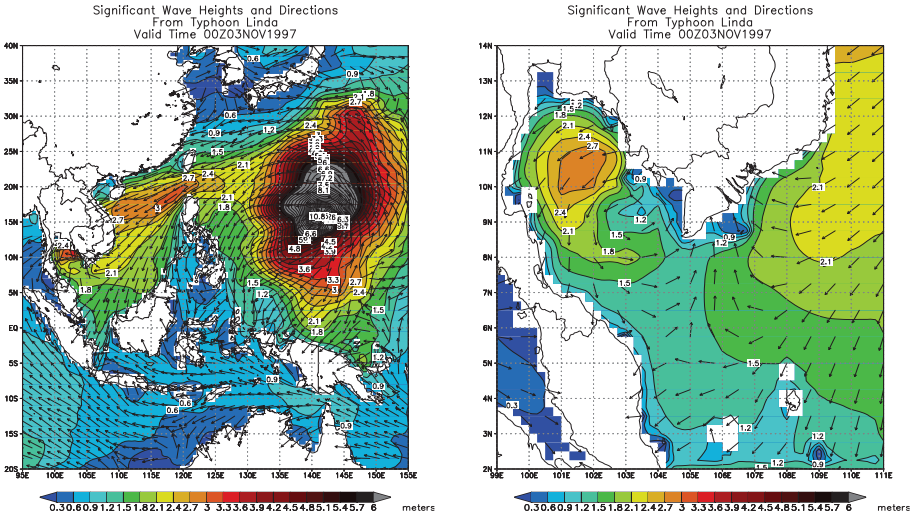

(a) (b)

Figure 5: The maximum significant wave height of Exp.I in (a) the CGD and (b) the FGD.

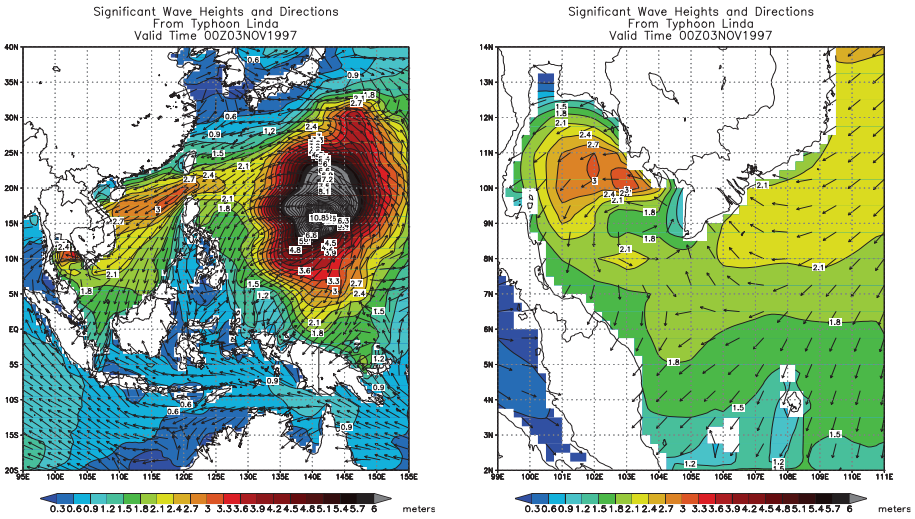

(a) (b)

Figure 6: The maximum significant wave height of Exp.II in (a) the CGD and (b) the FGD.

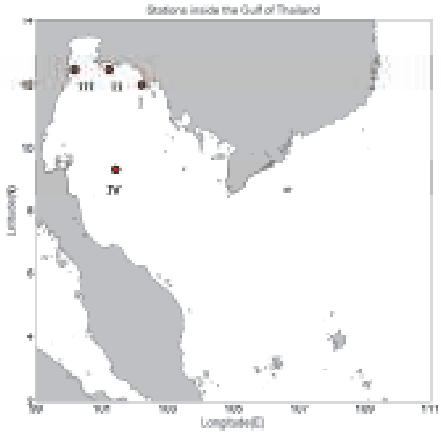

Figure 7: The observations in the study domain at buoy locations.

5 Discussions and Conclusion

The comparison of storm waves on the water surface layer of two experiments (Table 3) in the Typhoon Linda case exhibited that the wave height played a more significant role in determining the two–coordinates for energy balance equations by the WAMC4 model. The role of wave height can be clearly considered in Figure 8. Figure 8 and Table 3 showed the slight difference of wave height between Exp.I, Exp.II and observations (accept three in four stations for Exp.II) with typhoon distribution during Typhoon Linda entering into the GoT. The summary of WAMC4 model in four stations of Exp.II is shown in Figure 9. At Satun based weather station, the maximum wave height of approximately 12.5 m (Rogue wave at deep water) was affected by strong wind and wind gust. Additional studies will be investigated in the future with a focus on how storm waves affect other domain in the GoT. The effects of storm wave on the water surface layer should be more comprehensively examined with more typhoon case simulations. Additionally, the observational data are needed to calibrate and validate the models.

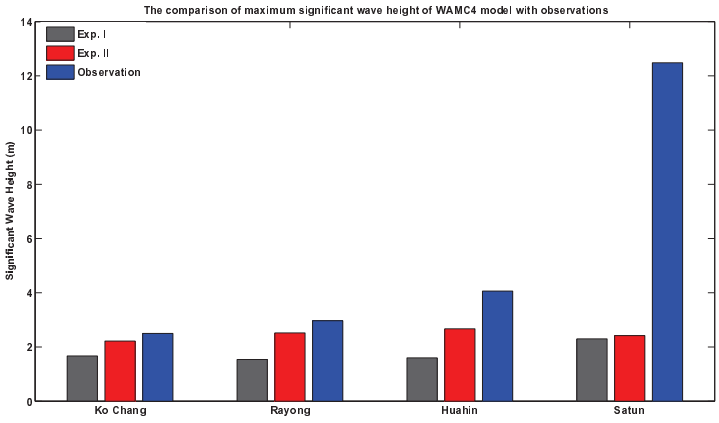

Figure 8: The comparison maximum of wave heights at each station.

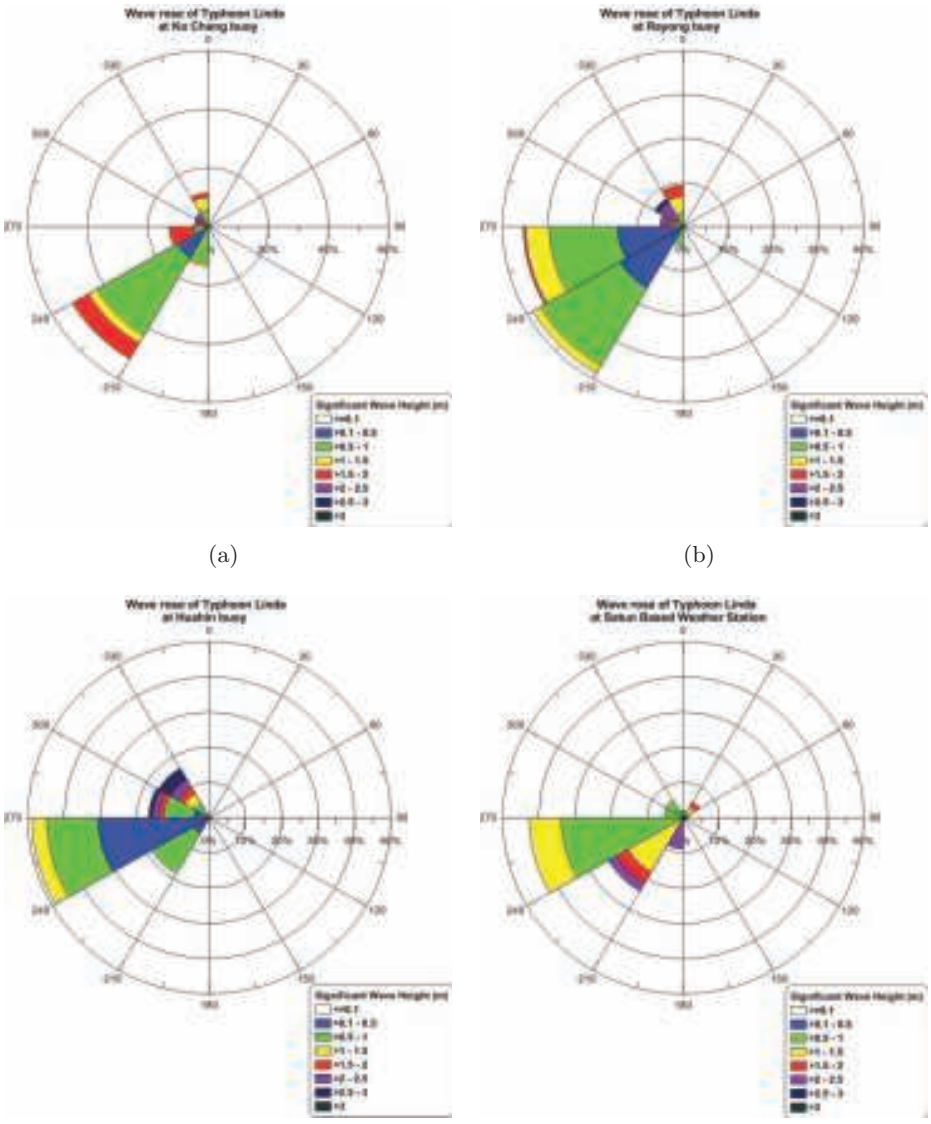

(a) (b)

(c) (d)

Figure 9: The summary of Exp.II of WAMC4 model in four stations (a) Ko Chang buoy, (b) Rayong buoy, (c) Huahin buoy and (d) Satun based weather station.

Acknowledgements. The authors would like to acknowledge the Commission on Higher Education for kindly providing financial support to Mr. Worachat Wannawong under the Strategic Scholarships Fellowships Frontier Research Networks (CHE–PhD–THA–NEU) in 2007. The authors are grateful to the Geo–Informatics and Space Technology Development Agency (Public Organization) (GISTDA) for buoy data and documents. The authors also wish to thank the Meteorological Division, Hydrographic Department, Royal Thai Navy, Sattahip, Chonburi, Thailand, for kindly providing laboratory space. Finally, the authors are greatly indebted to Mr. Michael Willing for helpful comments on English grammar and usage.

References

[1] C. Amante and B. W. Eakins, ETOPO1, 1 Arc–Minute Global Relief Model: Procedures, Data Sources and Analysis, NOAA, National Geophysical Data Center, Boulder, Colorado, U.S.A. (2008), 21.

[2] G. J. Komen, K. Hasselmann and S. Hasselmann, On the existence of a fully developed windsea spectrum, Journal of Physical Oceanography, 14(1984), 1271–1285.

[3] G. Komen, L. Cavaleri, M. Donelan, K. Hasselmann, S. Hasselmann and P.A.E.M. Janseen, Dynamics and Modelling of Ocean Waves, Cambridge University Press, UK. (1994), 532.

[4] G. Ph. van Vledder, Directional response of wind waves to turning winds, Commun. Hydraul. Geotech. Eng., Delft University of Technology, The Netherlands, 1990.

[5] H. Gunther, S. Hasselmann and P.A.E.M. Janssen, WAM model Cycle 4, Technical Report No. 4, Hamburg, Germany, 1992.

[6] H. L. Tolman, Wind wave propagation in tidal seas, Commun. Hydraul. Geotech. Eng., Delft University of Technology, The Netherlands, 1990.

[7] J. Monbaliu, R. Padilla–Hernandez, J. C. Hargreaves, J. C. Carretero–Albiach, W. Luo, M. Sclavo and H. Gunther, The spectral wave model WAM adapted for applications with high spatial resolution, Coastal Engineering, 41(2000), 4–62.

[8] K. Hasselmann, T. P. Barnett, E. Bouws, H. Carlson, D. E. Cartwright, K. Enke, J. I. Ewing, H. Gienapp, D. E. Hasselmann, P. Kruseman, A. Meerbrug, P. Mauller, D. J. Olvers, K. Richter, W. Sell and H. Walden, Measurements of wind–wave growth and swell decay during the Joint North Sea Wave Project (JONSWAP), Deutsche Hydrographische Zeitschrift, 8(1973), 95.

[9] M. O. Edwards, Global Gridded Elevation and Bathymetry on 5–Minute Geographic Grid (ETOPO5), NOAA, National Geophysical Data Center, Boulder, Colorado, U.S.A., 1989.

[10] M. Xia, L. Xie, L. J. Pietrafesa and M. Peng, A numerical study of storm surge in the cape fear river estuary and adjacent coast, Journal of Coastal Research, 24(2008), 159–167.

[11] P.A.E.M. Janssen, Quasi–linear theory of wind–wave generation applied to wave forecasting, Journal of Physical Oceanography, 19(1991), 745–754.

[12] P. A. Wittmann and P. D. Farrar, Global, regional and coastal wave prediction, Marine Technology Society Journal, 31(1997), 76–82.

[13] P. H. LeBlond and L. A. Mysak, Waves in the ocean. Elsevier, Amsterdam, 1978.

[14] S. Hasselmann, K. Hasselmann, E. Bauer, P.A.E.M. Janssen, G. J. Komen, L. Bertotti, P. Lionello, A. Guillaume, V. C. Cardone, J. A. Greenwood, M. Reistad, L. Zambresky and J. A. Ewing, The WAM model–a third generation ocean wave prediction model, Journal of Physical Oceanography, 18(1988), 1775–1810.

[15] S. Hasselmann, K. Hasselmann, J. H. Allender and T. P. Barnett, Computations and parameterizations of the nonlinear energy transfer in a gravity-wave spectrum, Part II: Parameterizations of the nonlinear energy transfer for application in wave models, Journal of Physical Oceanography, 15(1985), 1378–1391.

[16] S. Vongvisessomjai, Impacts of Typhoon Vae and Linda on wind waves in the upper gulf of Thailand and east coast, Songklanakarin Journal of Science and Technology, 29(2007), 1199–1216.

[17] S. Vongvisessomjai, Tropical cyclone disasters in the Gulf of Thailand, Songklanakarin Journal of Science and Technology, 31(2009), 213–227.

[18] T. F. Hogan and T. E. Rosmond, The description of the Navy Operational Global Atmospheric System's spectral forecast model, Monthly Weather Review, 119(1991), 1786–1815.

[19] W. Wannawong, U. W. Humphries and A. Luadsong, The application of curvilinear coordinate for primitive equation in the Gulf of Thailand, Thai Journal of Mathematics, 6(2008), 89–108.

(Received 16 November 2009)

W. Wannawong[†] and U.W. Humphries
Department of Mathematics
Faculty of Science
King Mongkut's University of Technology Thonburi
Bangkok 10140, THAILAND.
e-mail: worachataj@hotmail.com and usa.wan@kmutt.ac.th

P. Wongwises
The Joint Graduate School of Energy and Environment
King Mongkut's University of Technology Thonburi
Bangkok 10140, THAILAND.
e-mail: prungchan.won@kmutt.ac.th

S. Vongvisessomjai
Water and Environment Expert
TEAM Consulting Engineering and Management Co., Ltd.
151 TEAM Building Nuan Chan Road, Klong Kum, Bueng Kum
Bangkok 10230, THAILAND.
e-mail: suphat@team.co.th

W. Lueangaram
Meteorological Division, Hydrographic Department
Royal Thai Navy, Sattahip
Chonburi 20180, THAILAND.
e-mail: viriya.navy@gmail.com